A Minkowski Sum Interval Analysis Approach for Planar Arrays Sensitivity Analysis

L. Tenuti, N. Anselmi, P. Rocca, M. Salucci, and A. Massa

Abstract

In this work, the analysis the excitation tolerances on the radiation performances of planar phased arrays is dealt with. An innovative sensitivity tool is proposed, based on interval arithmetic and the Minkowski sum. Narrow but inclusive bounds can be analytically derived on the radiation pattern starting from the tolerances on the array excitations (both in amplitude and in phase). Moreover, thanks to the Minkowski sum, narrower intervals are estimated with respect to standard interval analysis (*IA*) tools based on the Cartesian rules. Some numerical results are shown, in order to verify the effectiveness of the developed approach, by analyzing planar arrays of different sizes.

1 Numerical Assessment - Analysis vs Number of Radiating Element $N \times M$

GOAL: This section considers the study of the influence of tolerances on the control points (in amplitude and phase) in planar array with different size. Accordingly, the test case considers different planar geometries, i.e, 8×6, 12×8, 16×8 and 20×10 elements for which the element excitations have been choosen to generate on the principals planes $u = 0$ and $v = 0$ a Dolph-Chebyshev pattern with SLL equal to -20 dB. The amplitude and phase tolerances have been choosen as: $\pm 0\%$, $\pm 10\%$ for the amplitude and ± 1, ± 5 and ± 10 $[deg]$ for the phase.

Array geometry:

- Uniform planar array: $N \times M = 8 \times 6$, $N \times M = 12 \times 8$, $N \times M = 16 \times 8$, $N \times M = 20 \times 10$.
- Inter-element spacing: $d_x = 0.5$ $[\lambda]$ - $d_y = 0.5$ $[\lambda]$;

Nominal control points:

- Separable distributions:
  - x-axis: Dolph-Chebyshev pattern: $SLL = 20$ $[dB]$.
  - y-axis: Dolph-Chebyshev pattern: $SLL = 20$ $[dB]$.

Tolerances on the control points:

- Amplitude tolerance: $\delta\alpha_n = \pm 0\,\%$, $\pm 10\,\%$.
- Phase tolerance: $\delta\beta_n = \pm 1$ $[deg]$, ± 5 $[deg]$, ± 10 $[deg]$.

Minkowski sum parameters:

- Number of sides including polygon: $L = 720$

1.1 Analysis vs NxM

1.1.1 Pattern Features - Interval Beamwidth

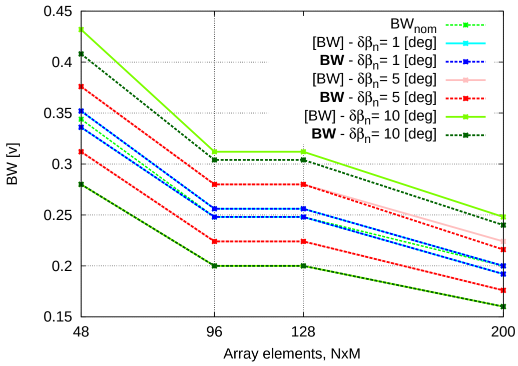

(a)

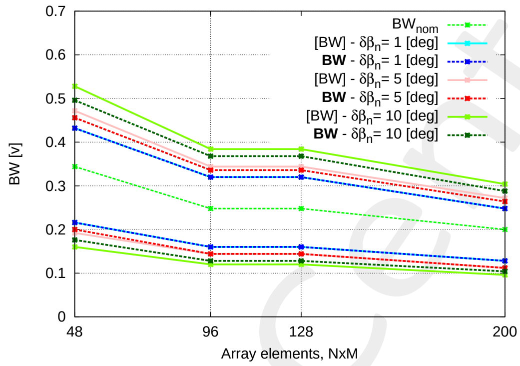

(b)

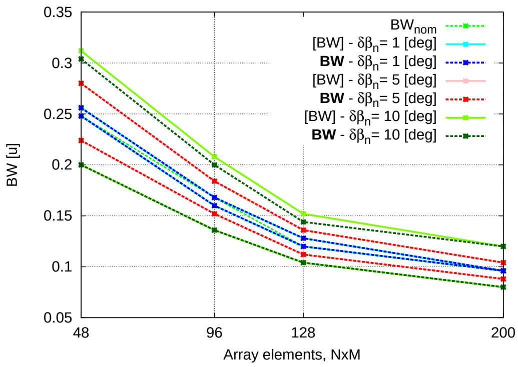

(c)

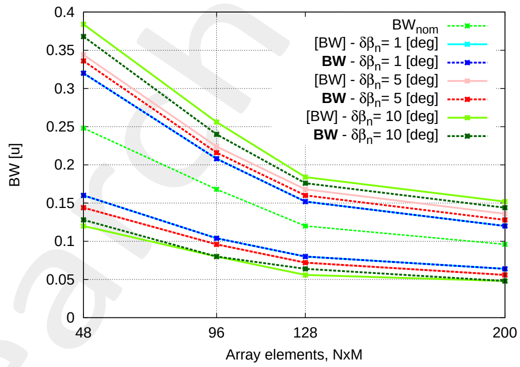

(d)

Table: Interval Beamwidth comparison Cartesian vs Minkowski sum

(a) $\delta\alpha_n = 0\%$ - plane $u = 0$, $(b)\delta\alpha_n = 10\%$ - plane $u = 0$

(c) $\delta\alpha_n = 0\%$ - plane $v = 0$, $(d)\delta\alpha_n = 10\%$ - plane $v = 0$

Amplitude Error: $\delta\alpha_n = 0\%$ **- Plane** $u = 0$

	Cartesian			*Minkowski*		
$N \times M/\delta\beta_n$ $[deg]$	1	5	10	1	5	10
48	[0.336, 0.352]	[0.312, 0.376]	[0.280, 0.432]	[0.336, 0.352]	[0.312, 0.376]	[0.280, 0.408]
96	[0.248, 0.256]	[0.224, 0.280]	[0.200, 0.312]	[0.248, 0.256]	[0.224, 0.280]	[0.200, 0.304]
128	[0.248, 0.256]	[0.224, 0.280]	[0.200, 0.312]	[0.248, 0.256]	[0.224, 0.280]	[0.200, 0.304]
200	[0.192, 0.200]	[0.176, 0.224]	[0.160, 0.248]	[0.192, 0.200]	[0.176, 0.216]	[0.160, 0.240]

Table: Interval Beamwidth vs $N \times M$ - $\delta\alpha_n = 0\%$ - Cartesian vs Minkowski sum

Amplitude Error: $\delta\alpha_n = 0\%$ **- Plane** $v = 0$

	Cartesian			*Minkowski*		
$N \times M/\delta\beta_n$ $[deg]$	1	5	10	1	5	10
48	[0.248, 0.256]	[0.224, 0.280]	[0.200, 0.312]	[0.248, 0.256]	[0.224, 0.280]	[0.200, 0.312]
96	[0.160, 0.168]	[0.152, 0.184]	[0.136, 0.208]	[0.160, 0.168]	[0.152, 0.184]	[0.136, 0.208]
128	[0.120, 0.128]	[0.112, 0.136]	[0.104, 0.152]	[0.120, 0.128]	[0.112, 0.136]	[0.104, 0.152]
200	[0.096, 0.0.096]	[0.088, 0.104]	[0.080, 0.120]	[0.096, 0.0.096]	[0.088, 0.0.104]	[0.080, 0.0.120]

Table: Interval Beamwidth vs $N \times M$ - $\delta\alpha_n = 0\%$ - Cartesian vs Minkowski sum

Amplitude Error: $\delta\alpha_n = 10\%$ **- Plane** $u = 0$

	Cartesian			*Minkowski*		
$N \times M/\delta\beta_n$ $[deg]$	1	5	10	1	5	10
48	[0.216, 0.432]	[0.192, 0.472]	[0.160, 0.528]	[0.216, 0.432]	[0.200, 0.456]	[0.176, 0.496]
96	[0.160, 0.320]	[0.144, 0.344]	[0.120, 0.384]	[0.160, 0.320]	[0.144, 0.336]	[0.128, 0.368]
128	[0.160, 0.320]	[0.144, 0.344]	[0.120, 0.384]	[0.160, 0.320]	[0.144, 0.336]	[0.128, 0.368]
200	[0.128, 0.248]	[0.112, 0.272]	[0.096, 0.304]	[0.128, 0.248]	[0.112, 0.264]	[0.104, 0.288]

Table: Interval Beamwidth vs $N \times M$ - $\delta\alpha_n = 10\%$ - Cartesian vs Minkowski sum

Amplitude Error: $\delta\alpha_n = 10\%$ **- Plane** $v = 0$

	Cartesian			*Minkowski*		
$N \times M/\delta\beta_n$ $[deg]$	1	5	10	1	5	10
48	[0.160, 0.320]	[0.144, 0.344]	[0.120, 0.384]	[0.160, 0.320]	[0.144, 0.336]	[0.128, 0.368]
96	[0.104, 0.208]	[0.096, 0.224]	[0.080, 0.256]	[0.104, 0.208]	[0.096, 0.216]	[0.080, 0.240]
128	[0.080, 0.152]	[0.072, 0.168]	[0.056, 0.184]	[0.080, 0.152]	[0.072, 0.160]	[0.064, 0.176]
200	[0.064, 0.120]	[0.056, 0.136]	[0.048, 0.152]	[0.064, 0.120]	[0.056, 0.128]	[0.048, 0.144]

Table: Interval Beamwidth vs $N \times M$ - $\delta\alpha_n = 0\%$ - Cartesian vs Minkowski

1.1.2 Pattern Features - Interval SLL

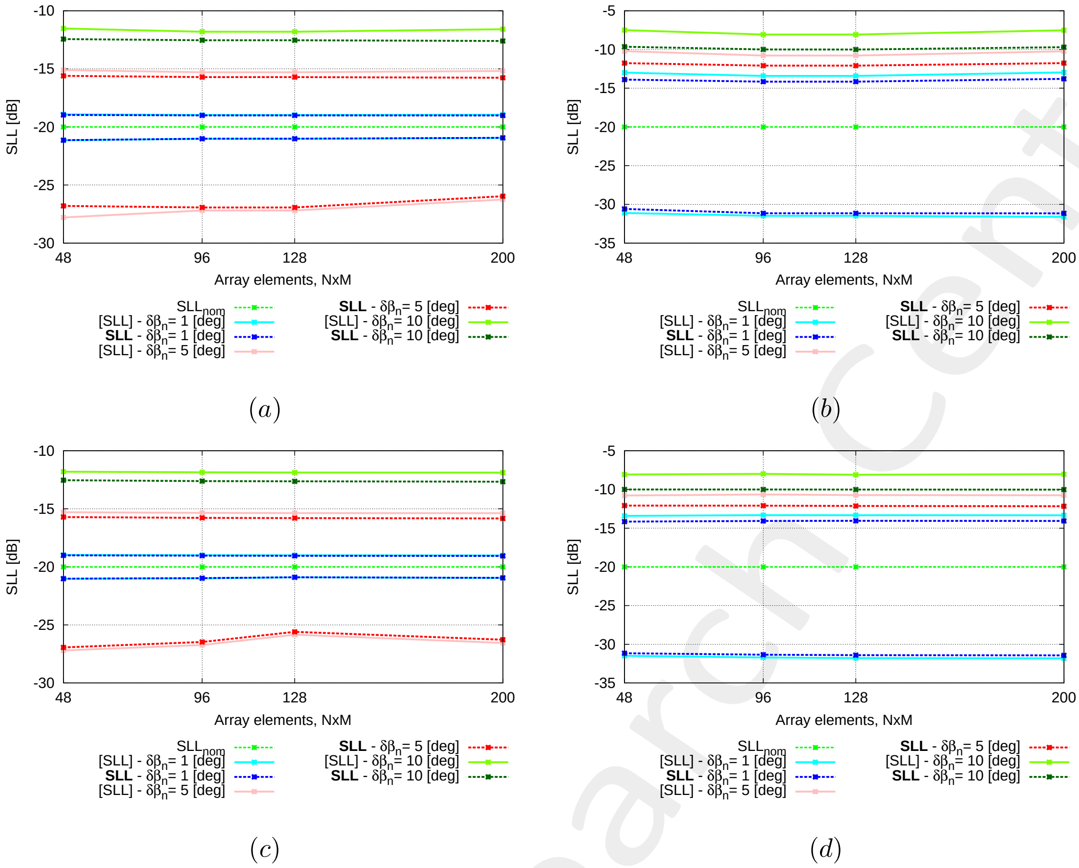

Table: Interval SLL comparison Cartesian vs Minkowski sum

(a) $\delta\alpha_n = 0\%$ - plane $u = 0$, $(b)\delta\alpha_n = 10\%$ - plane $u = 0$

(c) $\delta\alpha_n = 0\%$ - plane $v = 0$, $(d)\delta\alpha_n = 10\%$ - plane $v = 0$

Amplitude Error: $\delta\alpha_n = 0\%$ - Plane $u = 0$

	Cartesian			*Minkowski*		
$N \times M/\delta\beta_n$ $[deg]$	1	5	10	1	5	10
48	$[-21.15, -18.91]$	$[-27.79, -15.11]$	$[-\infty, -11.53]$	$[-21.14, -18.97]$	$[-26.80, -15.60]$	$[-\infty, -12.44]$
96	$[-21.02, -18.97]$	$[-27.19, -15.29]$	$[-\infty, -11.80]$	$[-21.01, -19.00]$	$[-26.94, -15.71]$	$[-\infty, -12.54]$
128	$[-21.02, -18.97]$	$[-27.19, -15.29]$	$[-\infty, -11.80]$	$[-21.01, -19.00]$	$[-26.94, -15.71]$	$[-\infty, -12.54]$
200	$[-20.95, -18.95]$	$[-26.25, -15.18]$	$[-\infty, -11.59]$	$[-20.94, -19.01]$	$[-25.97, -15.77]$	$[-\infty, -12.60]$

Table: Interval SLL vs $N \times M$ - $\delta\alpha_n = 0\%$ - Cartesian vs Minkowski sum

Amplitude Error: $\delta\alpha_n = 0\%$ **- Plane** $v = 0$

	Cartesian			*Minkowski*		
$N \times M/\delta\beta_n$ $[deg]$	1	5	10	1	5	10
48	$[-21.02,\ -18.97]$	$[-27.19,\ -15.29]$	$[-\infty,\ -11.80]$	$[-21.01,\ -19.00]$	$[-26.93,\ -15.71]$	$[-\infty,\ -12.54]$
96	$[-20.98,\ -18.99]$	$[-26.73,\ -15.35]$	$[-\infty,\ -11.86]$	$[-20.97,\ -19.00]$	$[-26.47,\ -15.78]$	$[-\infty,\ -12.61]$
128	$[-20.90,\ -19.00]$	$[-25.84,\ -15.37]$	$[-\infty,\ -11.88]$	$[-20.89,\ -19.04]$	$[-25.59,\ -15.80]$	$[-44.48,\ -12.63]$
200	$[-20.95,\ -19.01]$	$[-26.55,\ -15.38]$	$[-\infty,\ -11.88]$	$[-20.95,\ -19.06]$	$[-26.27,\ -15.83]$	$[-\infty,\ -12.66]$

Table: Interval SLL vs $N \times M$ - $\delta\alpha_n = 0\%$ - Cartesian vs Minkowski sum

Amplitude Error: $\delta\alpha_n = 10\%$ **- Plane** $u = 0$

	Cartesian			*Minkowski*		
$N \times M/\delta\beta_n$ $[deg]$	1	5	10	1	5	10
48	$[-31.12,\ -12.98]$	$[-\infty,\ -10.22]$	$[-\infty,\ -7.50]$	$[-30.59,\ -13.89]$	$[-\infty,\ -11.76]$	$[-\infty,\ -9.64]$
96	$[-31.49,\ -13.41]$	$[-\infty,\ -10.78]$	$[-\infty,\ -8.06]$	$[-31.16,\ -14.16]$	$[-\infty,\ -12.08]$	$[-\infty,\ -9.99]$
128	$[-31.49,\ -13.41]$	$[-\infty,\ -10.78]$	$[-\infty,\ -8.06]$	$[-31.16,\ -14.16]$	$[-\infty,\ -12.08]$	$[-\infty,\ -10.0]$
200	$[-31.62,\ -12.96]$	$[-\infty,\ -10.23]$	$[-\infty,\ -7.51]$	$[-31.16,\ -13.80]$	$[-\infty,\ -11.76]$	$[-\infty,\ -9.70]$

Table: Interval SLL vs $N \times M$ - $\delta\alpha_n = 10\%$ - Cartesian vs Minkowski sum

Amplitude Error: $\delta\alpha_n = 10\%$ **- Plane** $v = 0$

	Cartesian			*Minkowski*		
$N \times M/\delta\beta_n$ $[deg]$	1	5	10	1	5	10
48	$[-31.49,\ -13.41]$	$[-\infty,\ -10.78]$	$[-\infty,\ -8.06]$	$[-31.15,\ -14.16]$	$[-\infty,\ -12.08]$	$[-\infty,\ -10.00]$
96	$[-31.70,\ -13.32]$	$[-\infty,\ -10.65]$	$[-\infty,\ -7.99]$	$[-31.34,\ -14.07]$	$[-\infty,\ -12.10]$	$[-\infty,\ -10.00]$
128	$[-31.78,\ -13.32]$	$[-\infty,\ -10.72]$	$[-\infty,\ -8.09]$	$[-31.40,\ -14.05]$	$[-\infty,\ -12.13]$	$[-\infty,\ -10.01]$
200	$[-31.81,\ -13.34]$	$[-\infty,\ -10.75]$	$[-\infty,\ -8.03]$	$[-31.42,\ -14.07]$	$[-\infty,\ -12.17]$	$[-\infty,\ -10.02]$

Table: Interval SLL vs $N \times M$ - $\delta\alpha_n = 0\%$ - Cartesian vs Minkowski

1.1.3 Pattern Features - Interval Power Peak - $(u, v) = (0, 0)$

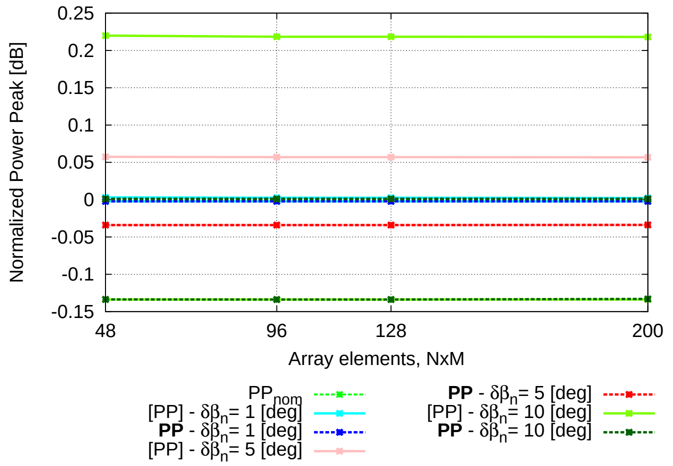

(a)

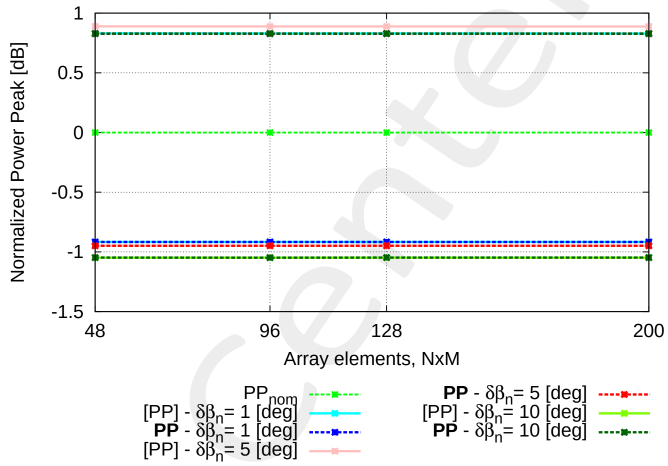

(b)

Table: Interval PP comparison Cartesian vs Minkowski sum

(a) $\delta\alpha_n = 0\%$, $(b)\delta\alpha_n = 10\%$

Amplitude Error: $\delta\alpha_n = 0\%$

	Cartesian			*Minkowski*		
$N \times M/\delta\beta_n$ $[deg]$	1	5	10	1	5	10
48	$[-2.19,\ 3.08] \times 10^{-3}$	$[-3.39,\ 5.75] \times 10^{-2}$	$[-1.33,\ 2.20] \times 10^{-1}$	$[-2.19,\ 0.0] \times 10^{-3}$	$[-3.39,\ 0.0] \times 10^{-2}$	$[-1.33,\ 0.0] \times 10^{-1}$
96	$[-2.19,\ 2.60] \times 10^{-3}$	$[-3.39,\ 5.70] \times 10^{-2}$	$[-1.33,\ 2.18] \times 10^{-1}$	$[-2.19,\ 0.0] \times 10^{-3}$	$[-3.39,\ 0.0] \times 10^{-2}$	$[-1.33,\ 0.0] \times 10^{-1}$
128	$[-2.19,\ 2.60] \times 10^{-3}$	$[-3.39,\ 5.70] \times 10^{-2}$	$[-1.33,\ 2.18] \times 10^{-1}$	$[-2.19,\ 0.0] \times 10^{-3}$	$[-3.39,\ 0.0] \times 10^{-2}$	$[-1.33,\ 0.0] \times 10^{-1}$
200	$[-2.19,\ 2.19] \times 10^{-3}$	$[-3.39,\ 5.70] \times 10^{-2}$	$[-1.33,\ 2.20] \times 10^{-1}$	$[-2.19,\ 0.0] \times 10^{-3}$	$[-3.39,\ 0.0] \times 10^{-2}$	$[-1.33,\ 0.0] \times 10^{-1}$

Table: Interval PP vs $N \times M$ - $\delta\alpha_n = 0\%$ - Cartesian vs Minkowski sum

Amplitude Error: $\delta\alpha_n = 10\%$

	Cartesian			*Minkowski*		
$N \times M/\delta\beta_n$ $[deg]$	1	5	10	1	5	10
48	$[-0.91,\ 0.83]$	$[-0.95,\ 0.89]$	$[-1.05,\ 1.06]$	$[-0.91,\ 0.83]$	$[-0.95,\ 0.83]$	$[-1.05,\ 0.83]$
96	$[-0.91,\ 0.83]$	$[-0.95,\ 0.89]$	$[-1.05,\ 1.06]$	$[-0.91,\ 0.83]$	$[-0.95,\ 0.83]$	$[-1.05,\ 0.83]$
128	$[-0.91,\ 0.83]$	$[-0.95,\ 0.89]$	$[-1.05,\ 1.06]$	$[-0.91,\ 0.83]$	$[-0.95,\ 0.83]$	$[-1.05,\ 0.83]$
200	$[-0.91,\ 0.83]$	$[-0.95,\ 0.89]$	$[-1.05,\ 1.06]$	$[-0.91,\ 0.83]$	$[-0.95,\ 0.83]$	$[-1.05,\ 0.83]$

Table: Interval PP vs $N \times M$ - $\delta\alpha_n = 10\%$ - Cartesian vs Minkowski sum

1.1.4 Pattern Features - Pattern Tolerance Δ

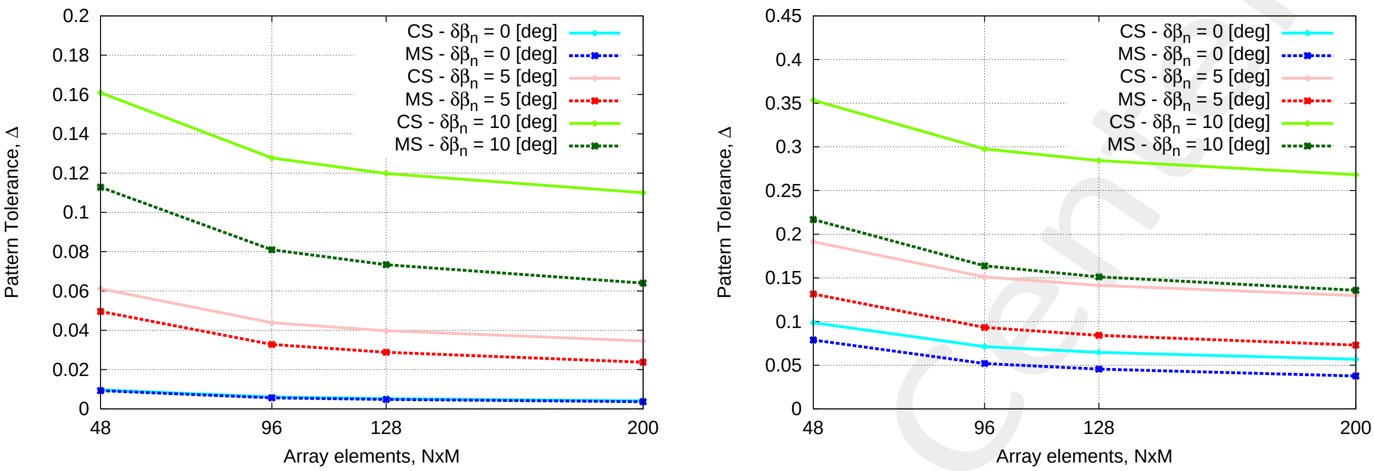

Table: Pattern Matching comparison Cartesian vs Minkowski sum

$(a)\ \delta\alpha_n = 0\%,\ (b)\delta\alpha_n = 10\%$

Amplitude Error: $\delta\alpha_n = 0\%$

	Cartesian			*Minkowski*		
$N \times M/\delta\beta_n$ [deg]	1	5	10	1	5	10
48	9.66×10^{-3}	6.11×10^{-2}	1.61×10^{-1}	9.28×10^{-3}	4.96×10^{-2}	1.12×10^{-1}
96	6.05×10^{-3}	4.39×10^{-2}	1.27×10^{-1}	5.65×10^{-3}	3.28×10^{-2}	0.81×10^{-1}
128	5.19×10^{-3}	3.97×10^{-2}	1.19×10^{-1}	4.78×10^{-3}	2.88×10^{-2}	0.73×10^{-1}
200	4.07×10^{-3}	3.46×10^{-2}	1.10×10^{-1}	3.68×10^{-3}	2.37×10^{-2}	0.64×10^{-1}

Table: Pattern Tolerance Δ vs $N \times M$ - $\delta\alpha_n = 0\%$ - Cartesian vs Minkowski sum

Amplitude Error: $\delta\alpha_n = 10\%$

	Cartesian			*Minkowski*		
$N \times M/\delta\beta_n$ [deg]	1	5	10	1	5	10
48	9.87×10^{-2}	1.91×10^{-1}	3.53×10^{-1}	7.89×10^{-2}	1.31×10^{-1}	2.16×10^{-1}
96	7.12×10^{-2}	1.51×10^{-1}	2.97×10^{-1}	5.19×10^{-2}	0.93×10^{-1}	1.63×10^{-1}
128	6.47×10^{-2}	1.41×10^{-1}	2.84×10^{-1}	4.55×10^{-2}	0.84×10^{-1}	1.51×10^{-1}
200	5.68×10^{-2}	1.29×10^{-1}	2.68×10^{-1}	3.77×10^{-2}	0.73×10^{-1}	1.36×10^{-1}

Table: Pattern Tolerance Δ vs $N \times M$ - $\delta\alpha_n = 10\%$ - Cartesian vs Minkowski sum

1.1.5 Pattern Features - Normalized Pattern Tolerance Δ_{norm}

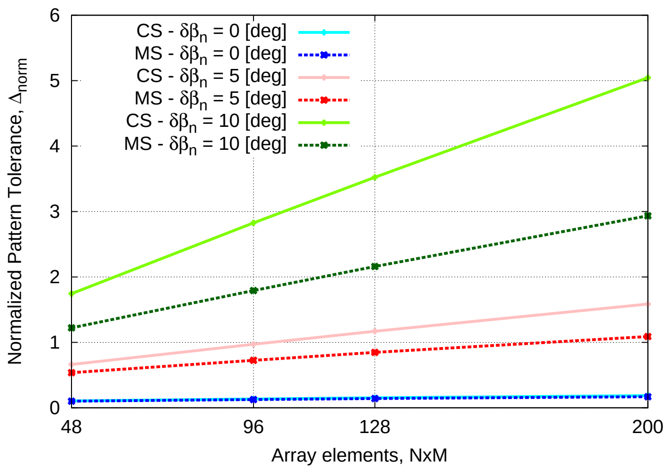

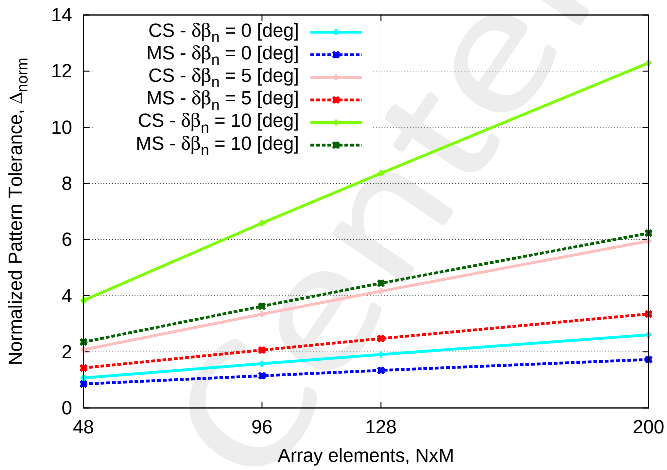

Table: Normalized Pattern Tolerance Δ_{norm} comparison

Cartesian vs Minkowski sum (a) $\delta\alpha_n = 0\%$, $(b)\delta\alpha_n = 10\%$

Amplitude Error: $\delta\alpha_n = 0\%$

	Cartesian			*Minkowski*		
$N \times M/\delta\beta_n$ $[deg]$	1	5	10	1	5	10
48	0.105	0.662	1.743	0.100	0.537	1.222
96	0.134	0.970	2.827	0.125	0.725	1.792
128	0.152	1.170	3.523	0.141	0.846	2.159
200	0.187	1.586	5.045	0.169	1.089	2.934

Table: Δ_{norm} vs $N \times M$ - $\delta\alpha_n = 0\%$ - Cartesian vs Minkowski sum

Amplitude Error: $\delta\alpha_n = 10\%$

	Cartesian			*Minkowski*		
$N \times M/\delta\beta_n$ $[deg]$	1	5	10	1	5	10
48	1.070	2.074	3.830	0.855	1.425	2.349
96	1.577	3.343	6.588	1.149	2.065	3.627
128	1.905	4.160	8.363	1.339	2.475	4.447
200	2.604	5.949	12.29	1.728	3.348	6.228

Table: Δ_{norm} vs $N \times M$ - $\delta\alpha_n = 10\%$ - Cartesian vs Minkowski sum

1.1.6 Comments and Observations:

When increasing the number of radiating elements, the normalize pattern tolerance Δ_{norm} increases.This means that in large arrays the deviation from the nominal pattern is grater than in small arrays. However, this not affect to much the pattern features (more specifically the SLL and PP losses), that seem to be almost constant with respect to number of radiating elements.

References

[1] N. Anselmi, P. Rocca, M. Salucci, and A. Massa, "Optimization of excitation tolerances for robust beamforming in linear arrays," *IET Microw. Antennas Propag.*, vol. 10, no. 2, pp. 208-214, 2016.

[2] P. Rocca, G. Oliveri, R. J. Mailloux, and A. Massa, "Unconventional phased array architectures and design Methodologies - A review," *Proc. IEEE*, vol. 104, no. 3, pp. 544-560, Mar. 2016.

[3] G. Oliveri, M. Salucci, and A. Massa, "Synthesis of modular contiguously clustered linear arrays through a sparseness-regularized solver," *IEEE Trans. Antennas Propag,*, vol. 64, no. 10, pp. 4277-4287, Oct. 2016.

[4] L. Poli, P. Rocca, N. Anselmi, and A. Massa, "Dealing with uncertainties on phase weighting of linear antenna arrays by means of interval-based tolerance analysis," *IEEE Trans. Antennas Propag.*, vol. 63, no. 7, pp. 3299-3234, Jul. 2015.

[5] P. Rocca, N. Anselmi, and A. Massa, "Optimal synthesis of robust beamformer weights exploiting interval analysis and convex optimization," *IEEE Trans. Antennas Propag.*, vol. 62, no. 7, pp. 3603-3612, Jul. 2014.

[6] L. Manica, N. Anselmi, P. Rocca, and A. Massa, "Robust mask-constrained linear array synthesis through an interval-based particle swarm optimisation," *IET Microw. Antennas Propag.*, vol. 7, no. 12, pp. 976-984, Sep. 2013.

[7] N. Anselmi, L. Manica, P. Rocca, and A. Massa, "Tolerance analysis of antenna arrays through interval arithmetic," *IEEE Trans. Antennas Propag.*, vol. 61, no. 11, pp. 5496-5507, Nov. 2013.

[8] P. Rocca, L. Manica, N. Anselmi, and A. Massa, "Analysis of the pattern tolerances in linear arrays with arbitrary amplitude errors," *IEEE Antennas Wireless Propag. Lett.*, vol. 12, pp. 639-642, 2013.

[9] T. Moriyama, L. Poli, N. Anselmi, M. Salucci, and P. Rocca, "Real array pattern tolerances from amplitude excitation errors," *IEICE Electron. Express*, vol. 11, no. 17, pp. 1-8, Sep. 2014.

[10] P. Rocca, N. Anselmi, and A. Massa, "Optimal synthesis of robust array configurations exploiting interval analysis and convex optimization," *IEEE Trans. Antennas Propag.*, vol. 62, no. 7, pp. 3603-3612, Jul. 2014.

[11] N. Anselmi, P. Rocca, M. Salucci, and A. Massa, "Power pattern sensitivity to calibration errors and mutual coupling in linear arrays through circular interval arithmetics," *Sensors*, vol. 16, no. 6 (791), pp. 1-14, 2016.

[12] L. Tenuti, N. Anselmi, P. Rocca, M. Salucci, and A. Massa, "Minkowski sum method for planar arrays sensitivity analysis with uncertain-but-bounded excitation tolerances," *IEEE Trans. Antennas Propag.*, vol. 65, no. 1, pp. 167-177, Jan. 2017.

[13] P. Rocca, N. Anselmi, and A. Massa, "Interval Arithmetic for pattern tolerance analysis of parabolic reflectors," *IEEE Trans. Antennas Propag.*, vol. 62, no. 10, pp. 4952-4960, Oct. 2014.

[14] P. Rocca, L. Poli, N. Anselmi, M. Salucci, and A. Massa, "Predicting antenna pattern degradations in microstrip reflectarrays through interval arithmetic," *IET Microw. Antennas Propag.*, vol. 10, no. 8, pp. 817-826, May 2016.

[15] N. Anselmi, M. Salucci, P. Rocca, and A. Massa, "Generalized sensitivity analysis tool for pattern distortions in reflector antennas with bump-like surface deformations," *IET Microw. Antennas Propag.*, vol. 10, no. 9, p. 909-916, Jun. 2016.